IEEE Access
Multidisciplinary | Rapid Review | Open Access Journal

Date of publication xxxx 00, 2018, date of current version January 4, 2018.

Digital Object Identifier xxxxyyyyzzzz

Equalization techniques of control and non-payload communication links for unmanned aerial vehicles

DONATELLA DARSENA[1], (Senior Member, IEEE), GIACINTO GELLI[2], IVAN IUDICE[3], AND FRANCESCO VERDE[2], (Senior Member, IEEE)

[1]Department of Engineering, Parthenope University, Naples I-80143, Italy (e-mail: darsena@uniparthenope.it)
[2]Department of Electrical Engineering and Information Technology, University Federico II, Naples I-80125, Italy (e-mail: [gelli, f.verde]@unina.it)
[3]Communication Systems Laboratory, Italian Aerospace Research Centre (CIRA), Capua I-81043, Italy (e-mail: i.iudice@cira.it)

Corresponding author: Giacinto Gelli (e-mail: gelli@unina.it).

This work was supported by CeSMA project "Advanced signal processing and optimization techniques for information and power sources". The work of I. Iudice was partially supported by the CIRA project "TECVOL-II".

ABSTRACT In the next years, several new applications involving unmanned aerial vehicles (UAVs) for public and commercial uses are envisaged. In such developments, since UAVs are expected to operate within the public airspace, a key issue is the design of reliable control and non-payload communication (CNPC) links connecting the ground control station to the UAV. At the physical layer, CNPC design must cope with time- and frequency-selectivity (so-called double selectivity) of the wireless channel, due to low-altitude operation and flight dynamics of the UAV. In this paper, we consider the transmission of continuous phase modulated (CPM) signals for UAV CNPC links operating over doubly-selective channels. Leveraging on the Laurent representation for a CPM signal, we design a two-stage receiver: the first one is a linear time-varying (LTV) equalizer, synthesized under either the zero-forcing (ZF) or minimum mean-square error (MMSE) criterion; the second one recovers the transmitted symbols from the pseudo-symbols of the Laurent representation in a simple recursive manner. In addition to LTV-ZF and LTV-MMSE equalizers, their widely-linear versions are also developed, to take into account the possible noncircular features of the CPM signal. Moreover, relying on a basis expansion model (BEM) of the doubly-selective channel, we derive frequency-shift versions of the proposed equalizers, by discussing their complexity issues and proposing simplified implementations. Monte Carlo numerical simulations show that the proposed receiving structures are able to satisfactorily equalize the doubly-selective channel in typical UAV scenarios.

INDEX TERMS Basis expansion channel models, continuous phase modulation, control and non-payload communication links, doubly-selective channels, time-varying equalization.

I. INTRODUCTION

AFTER their introduction in the military field, the use of *unmanned aerial vehicles (UAVs)*, also commonly referred as *drones*, is expected to grow dramatically in the coming decades for many civilian applications, including monitoring, surveillance, traffic control, remote sensing, communications relaying, agriculture, and shipping [1]–[3]. In these operative scenarios, the bidirectional channel connecting the remote pilot located at a ground control facility with the UAV in the airspace represents a safety-critical communication connection [3], which is referred to as the *control and non-payload communication* (CNPC) link. The design of CNPC systems for UAV applications demands improved receiving structures, in order to satisfy higher requirements in terms of reliability, availability, and low latency, so as to ensure operation capabilities in a large variety of environmental and propagation conditions. As a reference, typical rate requirements [1] for an UAV CNPC link are in the order of $10-20$ Kbps in uplink and up to 270 Kbps in downlink (when a video stream is required for piloting aids). In this paper, we focus attention on the physical layer design of a CNPC link, which is a fundamental tool to implement networks of UAVs.

For years, there was a lack of approved national and international standards for designing CNPC links for UAV applications. Techniques compliant to the IRIG-106 telemetry standard [4], based on PCM/FM, were used for medium-

This article has been accepted for publication in a future issue of this journal, but has not been fully edited. Content may change prior to final publication. Citation information: DOI 10.1109/ACCESS.2018.2791098, IEEE Access

to-large dimension UAVs, whereas smaller vehicles typically employed inexpensive communication chips mostly based on the Gaussian minimum-shift keying (GMSK) modulation format. Recently, the Radio Technical Commission for Aeronautics (RTCA) started to develop requirements and standards for CNPC links [5]. To this aim, many transmission techniques were evaluated for UAV communications: among them, one of the preferred solution is GMSK, due to its many favorable properties, such as low power consumption, high spectral efficiency, and noise robustness.

GMSK belongs to the family of *continuous phase modulated* (CPM) [6] signals. Since CPM is a modulation with memory, its main drawback is the high computational complexity of the optimal maximum-likelihood (ML) detection strategy. This issue is tackled on the additive white Gaussian noise (AWGN) channel by exploiting the trellis structure of CPM and resorting to the Viterbi algorithm (VA) [7]. However, ML detection of CPM signals over frequency-selective channels is much more cumbersome, since the number of states of the extendend trellis grows exponentially with the channel length. Even worse, in CNPC links for UAV applications, due to flight dynamics and low-altitude operations, the wireless channel exhibits not only frequency selectivity, but also significant time selectivity, due to Doppler effects: when CPM modulations are employed over such *doubly-selective* channels, optimal ML detection becomes prohibitive, due to the huge number of states of the VA and the need to perform fast channel estimation and tracking.

Several approaches aimed at reducing the complexity of the ML detector have been proposed, mostly targeted at linear time-invariant (LTI) channels. A viable strategy [8]–[10] consists of performing preliminary channel equalization in the frequency domain, aimed at mitigating the effects of intersymbol interference (ISI), allowing thus the subsequent VA to work in an almost ISI-free setting, albeit with colored noise. However, frequency-domain equalization becomes cumbersome in the presence of high Doppler spreads, since in this case the time-varying channel cannot be diagonalized by a channel-independent transformation.

To devise efficient solutions for doubly-selective channel equalization, a parsimonious representation (i.e., with a small number of parameters) of the channel is required. A popular approach is the *basis expansion model* (BEM) [11], [12], wherein the channel impulse response (CIR) is expressed as a superposition of time-varying functions, such as complex exponentials (CEs), with time-invariant coefficients. BEM models with different basis functions have been employed in a number of communication applications, including diversity transmissions [12], channel shortening [13], [14], equalization [15]–[17], and channel identification [18], [19].

In this paper, we synthesize new equalization techniques for CPM signals to be employed in UAV CNPC links operating over doubly-selective wireless channels. In particular, when the CPM signal is circular or proper [20], we synthesize linear time-varying (LTV) zero-forcing (ZF) or minimum mean-square error (MMSE) equalizers. When instead the CPM signal exhibits noncircular or improper features, which interestingly happens for the GMSK format, we synthesize *widely-linear* [21] time-varying (WLTV) ZF or MMSE equalizers, which are expected to significantly outperform their LTV or LTI counterparts. The proposed synthesis leverages on Laurent decomposition [22] of a CPM signal, which allows one to obtain approximate but computationally-efficient versions of the devised equalizers. Moreover, by exploiting the CE-BEM of the doubly-selective channel, we derive convenient frequency-shift (FRESH) implementations [23] of the proposed receivers, which can be implemented as a parallel bank of LTI filters having, as input signals, different frequency-shifted and possibly conjugated versions of the received data. The performance of the proposed receiving structures is assessed by Monte Carlo computer simulations, for the interesting scenario of a GMSK-modulated CNPC link operating over a typical UAV wireless channel.

A. NOTATIONS

Besides standard notations, we adopt the following ones: $\mathbb{N}_0 \triangleq \mathbb{N} \cup \{0\}$; matrices [vectors] are denoted with upper [lower] case boldface letters (e.g., $\boldsymbol{A}$ or $\boldsymbol{a}$); $(\cdot)^*$, $(\cdot)^{\mathrm{T}}$, $(\cdot)^{\mathrm{H}}$, $(\cdot)^{-1}$, $(\cdot)^{-}$ denote the conjugate, the transpose, the Hermitian (conjugate transpose), the inverse, and the generalized (1)-inverse [24] of a matrix, respectively; $\boldsymbol{0}_m \in \mathbb{R}^m$, $\boldsymbol{O}_{m\times n} \in \mathbb{R}^{m\times n}$, and $\boldsymbol{I}_m \in \mathbb{R}^{m\times m}$ denote the null vector, the null matrix, and the identity matrix, respectively; $\otimes$ denotes the Kronecker product, $(\cdot)_R$ denotes the modulo-R operation, and $\mathbb{E}[\cdot]$ denotes ensemble averaging; $\mathrm{diag}\,[a_{11}, a_{22}, \ldots, a_{nn}]$ denotes a diagonal matrix wherein $\{a_{ii}\}_{i=1}^{n}$ are the diagonal entries, and $\boldsymbol{J}_n = \mathrm{diag}\left[1, -1, \ldots, (-1)^{n-1}\right] \in \mathbb{R}^{n\times n}$.

II. SYSTEM MODEL

Let us consider a wireless communication system employing CPM modulation with baud-rate $1/T$. By adopting a one-sided model, the complex envelope of the CPM signal for $t \geq 0$ can be written as

$$x_{\mathrm{a}}(t) = \exp\left[j2\pi h \sum_{n=0}^{+\infty} a_n\, g(t - nT) \right] \tag{1}$$

where h is the modulation index of the signal, the information-bearing symbol sequence $\{a_n\}_{n\geq 0}$ assumes values in the M-ary alphabet $A \triangleq \{\pm 1, \pm 3, \ldots, \pm(M-1)\}$, $g(t) \triangleq \int_0^t f(u)\,du$ is the *phase response*, and $f(t)$ is the *frequency response* satisfying the three conditions: $f(t) \equiv 0$ for each $t \notin [0, LT]$; $f(t) = f(LT - t)$; and $\int_0^{LT} f(u)\,du = g(LT) = 1/2$, with $L \in \mathbb{N}$. GMSK modulation is a particular case of (1) with $h = 1/2$ and a Gaussian-shaping $f(t)$ [6].

For non-integer h and $M = 2$ (binary CPM), the signal $x_{\mathrm{a}}(t)$ can be expressed [22] for $t \geq 0$ as a superposition of $Q \triangleq 2^{L-1}$

This article has been accepted for publication in a future issue of this journal, but has not been fully edited. Content may change prior to final publication. Citation information: DOI 10.1109/ACCESS.2018.2791098, IEEE Access

PAM waveforms[1] as follows

$$x_a(t) = \sum_{q=0}^{Q-1} \sum_{n=0}^{+\infty} s_{q,n}\, c_{\mathrm{a},q}(t-nT) \tag{2}$$

where, for $n \geq 0$ and $q \in \{0,1,\ldots,Q-1\}$, the following *nonlinear* functions of $\{a_n\}_{n\geq 0}$:

$$s_{q,n} = \exp\left[j\pi h \left(\sum_{\ell=0}^{n} a_\ell - \sum_{\ell=0}^{\min(n,L-1)} a_{n-\ell}\, \beta_{q,\ell} \right) \right] \tag{3}$$

are the *pseudo-symbols*, where $\beta_{q,\ell} \in \{0,1\}$, for $\ell \in \{1,2,\ldots,L-1\}$, is the ℓth bit of the radix-2 representation of q, i.e., $q = \sum_{\ell=1}^{L-1} 2^{\ell-1} \beta_{q,\ell}$ (with $\beta_{q,0} = 0$) and $c_{\mathrm{a},q}(t)$ is a real-valued pulse (see [22] for the detailed expression) obeying $c_{\mathrm{a},q}(t) \equiv 0$ for each $t \notin [0, L_q T]$, with $L_q \triangleq \min_{0\leq \ell \leq L-1}[L(2-\beta_{q,\ell}) - \ell] \leq L+1$.

The integer L represents the length of the frequency response, expressed in symbol periods: when $L = 1$ (*full response CPM*) one has $Q = 1$, that is, there is only one PAM component in (2); on the other hand, when $L > 1$ (*partial response CPM*), it results [26] that, for smooth phase response pulses, the power of $x_{\mathrm{a}}(t)$ is mainly contained in the first PAM component, i.e., the one associated with $c_{\mathrm{a},0}(t)$, which exhibits moreover the longest duration.

To obtain a compact discrete model for the overall communication system, we assume that the CPM signal is well represented by its samples $x(k) \triangleq x_{\mathrm{a}}(kT_{\mathrm{c}})$ taken with rate $1/T_{\mathrm{c}} \triangleq N/T$, with $N > 1$ denoting the *oversampling factor*. In particular, we will find it convenient to resort to the following *polyphase decomposition* [27] of $x(k)$ with respect to N:

$$x^{(\eta)}(\ell) \triangleq x(\ell N + \eta) = \sum_{q=0}^{Q-1} \sum_{i=0}^{+\infty} s_{q,i}\, c_q^{(\eta)}(\ell - i) \tag{4}$$

where (2) has been taken into account, and $c_q^{(\eta)}(\ell) \triangleq c_{\mathrm{a},q}(\ell T + \eta T_{\mathrm{c}})$, with $\eta \in \{0,1,\ldots,N-1\}$. The CPM signal given by (1) or (2) is up-converted to radio-frequency (RF) and transmitted over a wireless channel; the received distorted signal, corrupted by AWGN, is filtered and sampled.

Denoting with $h_{\mathrm{a}}(t,\tau)$ the overall time-varying CIR (including also the effects of transmit/receive filters), we assume that: **(a1)** $\forall t \in \mathbb{R}$, the channel spans L_{h} symbol periods in τ, i.e., $h_{\mathrm{a}}(t,\tau) \equiv 0$ for $\tau \notin [0, L_{\mathrm{h}} T]$. Hence, assuming perfect symbol synchronization, the complex envelope of the received signal, at the output of the receiver filter, can be expressed as

$$r_{\mathrm{a}}(t) = \sum_{\ell=0}^{+\infty} \sum_{\eta=0}^{N-1} x^{(\eta)}(\ell)\, h_{\mathrm{a}}(t, t-\ell T - \eta T_{\mathrm{c}}) + v_{\mathrm{a}}(t) \tag{5}$$

where $v_{\mathrm{a}}(t)$ is filtered AWGN and $x^{(\eta)}(\ell)$ is given by (4).

[1]The decomposition into PAM waveforms can be extended to multilevel CPM signaling by expressing the M-ary symbol sequence $\{a_n\}_{n\geq 0}$ in terms of binary subsequences [25]. Moreover, the pathological case of integer h can be dealt with by viewing $x_{\mathrm{a}}(t)$ as the product of CPM signals with rational modulation indices [25]. Therefore, generalization of the proposed equalization structures to $M > 2$ and/or integer h can be carried out with minor modifications.

The received signal (5) is sampled at time epochs $t_{k,\mu} \triangleq kT + \mu T_{\mathrm{c}}$, with $k \in \mathbb{Z}$ and $\mu \in \{0,1,\ldots,N-1\}$, thus obtaining $r^{(\mu)}(k) \triangleq r_{\mathrm{a}}(t_{k,\mu})$ represented by the following *polyphase decomposition* with respect to N:

$$r^{(\mu)}(k) = \sum_{\ell=0}^{L_{\mathrm{h}}} \sum_{\eta=0}^{N-1} h^{(\mu)}(k, \ell N + \mu - \eta)\, x^{(\eta)}(k-\ell) + v^{(\mu)}(k) \tag{6}$$

with $h^{(\mu)}(k,\ell) \triangleq h(kN+\mu, \ell)$, where the discrete-time channel $h(k,\ell) \triangleq h_{\mathrm{a}}(kT_{\mathrm{c}}, \ell T_{\mathrm{c}})$, due to **(a1)**, is a causal finite impulse response (FIR) system of order NL_{h}, i.e., $\forall k \in \mathbb{Z}$, $h(k,\ell) \equiv 0$ for $\ell \notin \{0,1,\ldots,NL_{\mathrm{h}}\}$, and $v^{(\mu)}(k) \triangleq v_{\mathrm{a}}(t_{k,\mu})$.

The following customary assumptions will be considered in the sequel: **(a2)** the symbols $a_n \in \{\pm 1\}$ are modeled as a sequence of independent and identically distributed (i.i.d.) zero-mean random variables, with $\mathbb{E}[a_n^2] = 1$; **(a3)** the noise samples $\{v^{(\mu)}(k)\}_{\mu=0}^{N-1}$ are modeled as mutually independent zero-mean i.i.d. complex circular random sequences, with variance $\sigma_v^2 \triangleq \mathbb{E}[|v^{(\mu)}(k)|^2]$, statistically independent of the symbol sequence $\{a_n\}_{n\geq 0}$. In what follows, we further assume that: **(a4)** the noise variance σ_v^2 is either exactly known at the receiver or it is estimated by using data-aided or non-data aided algorithms [28].

By gathering N consecutive samples (6) into the vector $\boldsymbol{r}(k) \triangleq [r^{(0)}(k), r^{(1)}(k), \ldots, r^{(N-1)}(k)]^{\mathrm{T}} \in \mathbb{C}^N$, model (6) can be compactly expressed as

$$\boldsymbol{r}(k) = \sum_{\ell=0}^{L_{\mathrm{h}}} \boldsymbol{H}_\ell(k)\, \boldsymbol{x}(k-\ell) + \boldsymbol{v}(k) \tag{7}$$

where, for $i_1, i_2 \in \{0,1,\ldots,N-1\}$,

$$\{\boldsymbol{H}_\ell(k)\}_{i_1,i_2} = h^{(i_1)}(k, \ell N + i_1 - i_2) \tag{8}$$

is the (i_1+1, i_2+1)th element of $\boldsymbol{H}_\ell(k) \in \mathbb{C}^{N\times N}$ and, due to (4) and the support properties [22] of $c_{a,q}(t)$, the vector $\boldsymbol{x}(k) \triangleq [x^{(0)}(k), x^{(1)}(k), \ldots, x^{(N-1)}(k)]^{\mathrm{T}} \in \mathbb{C}^N$ can be expressed as

$$\boldsymbol{x}(k) = \sum_{q=0}^{Q-1} \boldsymbol{C}_q\, \boldsymbol{s}_{q,k} \tag{9}$$

where, for $i_1 \in \{0,1,\ldots,N-1\}$ and $i_2 \in \{0,1,\ldots,L_q-1\}$,

$$\{\boldsymbol{C}_q\}_{i_1,i_2} = c_q^{(i_1)}(i_2) \tag{10}$$

is the (i_1+1, i_2+1)th element of $\boldsymbol{C}_q \in \mathbb{R}^{N\times L_q}$ and we have defined $\boldsymbol{s}_q(k) \triangleq [s_{q,k}, s_{q,k-1}, \ldots, s_{q,k-L_q+1}]^{\mathrm{T}} \in \mathbb{C}^{L_q}$.

III. TIME-VARYING DEMODULATION OF CPM SIGNALS

The proposed receiver exhibits a two-stage structure: the former stage performs LTV or WLTV channel equalization, allowing one to recover the pseudo-symbols

$$\boldsymbol{s}(n) \triangleq [s_{0,n}, s_{1,n}, \ldots, s_{Q-1,n}]^{\mathrm{T}} \tag{11}$$

the latter stage detects the sequence $\{a_n\}_{n\geq 0}$ by inverting the nonlinear mapping (3) between symbols and pseudo-symbols. Although the resulting overall structure is not optimal, it allows to equalize rapidly time-varying dispersive channels with an affordable complexity.

This article has been accepted for publication in a future issue of this journal, but has not been fully edited. Content may change prior to final publication. Citation information: DOI 10.1109/ACCESS.2018.2791098, IEEE Access

In the following, we separately describe LTV and WLTV channel equalization strategies.

A. FIRST STAGE: LTV CHANNEL EQUALIZATION

Consider first a causal FIR LTV equalizer of order $L_{\rm e} > 0$, whose input-output relationship, for any $k \in \mathbb{Z}$, is given by

$$\boldsymbol{y}(k) = \boldsymbol{F}^{\rm H}(k)\,\boldsymbol{z}(k) \tag{12}$$

where $\boldsymbol{F}(k) \in \mathbb{C}^{N(L_{\rm e}+1)\times Q}$ collects all the equalizer parameters, whereas

$$\boldsymbol{z}(k) \triangleq [\boldsymbol{r}^{\rm T}(k), \boldsymbol{r}^{\rm T}(k-1), \ldots, \boldsymbol{r}^{\rm T}(k-L_{\rm e})]^{\rm T} \in \mathbb{C}^{N(L_{\rm e}+1)} \tag{13}$$

is the equalizer input vector. By virtue of (9), one has

$$\begin{aligned}\boldsymbol{z}(k) &\triangleq \boldsymbol{H}(k) \sum_{q=0}^{Q-1} \overline{\boldsymbol{C}}_q \boldsymbol{b}_q(k) + \boldsymbol{w}(k) \\ &= \boldsymbol{H}(k)\overline{\boldsymbol{C}}\,\boldsymbol{b}(k) + \boldsymbol{w}(k)\end{aligned} \tag{14}$$

where $\boldsymbol{b}_q(k) \triangleq [s_{q,k}, s_{q,k-1}, \ldots, s_{q,k-L_{\rm a}-L_q+1}]^{\rm T} \in \mathbb{C}^{L_{\rm a}+L_q}$, with $L_{\rm a} \triangleq L_{\rm e} + L_{\rm h}$, $\overline{\boldsymbol{C}}_q \in \mathbb{R}^{N(L_{\rm a}+1)\times(L_{\rm a}+L_q)}$ is defined as

$$\overline{\boldsymbol{C}}_q \triangleq \begin{bmatrix} \boldsymbol{C}_q & \boldsymbol{0}_N & \cdots & \boldsymbol{0}_N \\ \boldsymbol{0}_N & \boldsymbol{C}_q & \cdots & \boldsymbol{0}_N \\ \vdots & \ddots & \ddots & \vdots \\ \boldsymbol{0}_N & \cdots & \boldsymbol{0}_N & \boldsymbol{C}_q \end{bmatrix} \tag{15}$$

$\boldsymbol{H}(k) \in \mathbb{C}^{N(L_{\rm e}+1)\times N(L_{\rm a}+1)}$ is the time-varying channel matrix,[2] whose expression is given in (15) at the top of the next page, and

$$\overline{\boldsymbol{C}} \triangleq [\overline{\boldsymbol{C}}_0, \overline{\boldsymbol{C}}_1, \ldots, \overline{\boldsymbol{C}}_{Q-1}] \in \mathbb{R}^{N(L_{\rm a}+1)\times(QL_{\rm a}+L_{\rm c})} \tag{16}$$

$$\boldsymbol{w}(k) \triangleq [\boldsymbol{v}^{\rm T}(k), \boldsymbol{v}^{\rm T}(k-1), \ldots, \boldsymbol{v}^{\rm T}(k-L_{\rm e})]^{\rm T} \in \mathbb{C}^{N(L_{\rm e}+1)} \tag{17}$$

$$\boldsymbol{b}(k) \triangleq [\boldsymbol{b}_0^{\rm T}(k), \boldsymbol{b}_1^{\rm T}(k), \ldots, \boldsymbol{b}_{Q-1}^{\rm T}(k)]^{\rm T} \in \mathbb{C}^{QL_{\rm a}+L_{\rm c}} \tag{18}$$

with $L_{\rm c} \triangleq \sum_{q=0}^{Q-1} L_q$. Let $d \in \{0, 1, \ldots, L_{\rm a}\}$ denote a suitable equalization delay, the LTV equalizer has to provide a reliable estimate of the pseudo-symbol block $\boldsymbol{s}(k-d)$. To this end, we present in the following two common strategies, i.e., the ZF and MMSE ones.

1) LTV-ZF equalizer

Imposing the ZF condition $\boldsymbol{y}(k) = \boldsymbol{s}(k-d)$ to (12) leads to the following system of linear equations:

$$\boldsymbol{F}^{\rm H}(k)\,\boldsymbol{H}(k)\,\overline{\boldsymbol{C}} = \boldsymbol{E}_d^{\rm T} \tag{19}$$

where $\boldsymbol{E}_d \in \mathbb{B}^{(QL_{\rm a}+L_{\rm c})\times Q}$ is given in (20) at the top of the following page, with

$$\boldsymbol{e}_{d,q} \triangleq [0, 0, \ldots, 0, 1, 0, 0, \ldots, 0]^{\rm T} \in \mathbb{B}^{L_q+L_{\rm a}} \tag{21}$$

having a one in the $(d+1)$th position, for any value of $q \in \{0, 1, \ldots, Q-1\}$. System (19) is consistent [24] if and only if $\overline{\boldsymbol{C}}^{\rm T}\boldsymbol{H}^{\rm H}(k)[\overline{\boldsymbol{C}}^{\rm T}\boldsymbol{H}^{\rm H}(k)]^{-}\boldsymbol{E}_d = \boldsymbol{E}_d$, $\forall k \in \mathbb{Z}$. If the time varying matrix $\boldsymbol{H}(k)\overline{\boldsymbol{C}} \in \mathbb{C}^{N(L_{\rm e}+1)\times(QL_{\rm a}+L_{\rm c})}$ is full-column rank, i.e., $\mathrm{rank}[\boldsymbol{H}(k)\overline{\boldsymbol{C}}] = QL_{\rm a}+L_{\rm c}$, $\forall k \in \mathbb{Z}$, it results that $\overline{\boldsymbol{C}}^{\rm T}\boldsymbol{H}^{\rm H}(k)[\overline{\boldsymbol{C}}^{\rm T}\boldsymbol{H}^{\rm H}(k)]^{-} = \boldsymbol{I}_{QL_{\rm a}+L_{\rm c}}$, $\forall k \in \mathbb{Z}$, and, then, the system (19) turns out to be consistent independently of the equalization delay d. In this case, the *minimal norm* solution of (19) is given (see, e.g., [24]) by

$$\boldsymbol{F}_{\rm ZF}(k) = \boldsymbol{H}(k)\overline{\boldsymbol{C}}[\overline{\boldsymbol{C}}^{\rm T}\boldsymbol{H}^{\rm H}(k)\boldsymbol{H}(k)\overline{\boldsymbol{C}}]^{-1}\boldsymbol{E}_d\,. \tag{22}$$

Since the condition $\mathrm{rank}[\boldsymbol{H}(k)\overline{\boldsymbol{C}}] = QL_{\rm a}+L_{\rm c}$, $\forall k \in \mathbb{Z}$, assures the consistency of the system (19) and, thus, the existence of the LTV-ZF equalizer, it seems natural to investigate the rank properties of $\boldsymbol{H}(k)\overline{\boldsymbol{C}}$. A necessary condition is that $QL_{\rm a}+L_{\rm c} = QL_{\rm h}+QL_{\rm e}+L_{\rm c} \le N(L_{\rm e}+1)$, from which

$$L_{\rm e} \ge \frac{QL_{\rm h}+L_{\rm c}-N}{N-Q}\,. \tag{23}$$

Equation (23) shows that oversampling ($N > 1$) is necessary to ensure the existence of a FIR ZF equalizer even when the CPM is full response (i.e., $Q = 1$): indeed, for $N = 1$, the inequality leading to (23) cannot be satisfied with a finite $L_{\rm e}$.

2) LTV-MMSE equalizer

For ill-conditioned channel matrices, ZF equalization can introduce moderate-to-high amount of noise enhancement. To counteract this phenomenon, we resort to the LTV-MMSE equalizer, whose expression can be obtained by minimizing the output mean-square error cost function

$$\mathrm{MSE}[\boldsymbol{F}(k)] \triangleq \mathbb{E}[\|\boldsymbol{y}(k) - \boldsymbol{s}(k-d)\|^2] \tag{24}$$

for all $k \in \mathbb{Z}$. It can be shown [29] that the optimal $\boldsymbol{F}(k)$ is given by

$$\boldsymbol{F}_{\rm MMSE}(k) = \boldsymbol{R}_{\boldsymbol{zz}}^{-1}(k)\boldsymbol{R}_{\boldsymbol{zs}}(k) \tag{25}$$

where $\boldsymbol{R}_{\boldsymbol{zz}}(k) \triangleq \mathbb{E}[\boldsymbol{z}(k)\boldsymbol{z}^{\rm H}(k)] \in \mathbb{C}^{N(L_{\rm e}+1)\times N(L_{\rm e}+1)}$ and $\boldsymbol{R}_{\boldsymbol{zs}}(k) \triangleq \mathbb{E}[\boldsymbol{z}(k)\boldsymbol{s}^{\rm H}(k-d)] \in \mathbb{C}^{N(L_{\rm e}+1)\times Q}$. By virtue of (14) and assumptions **(a2)**–**(a3)**, it can be readily obtained that

$$\boldsymbol{R}_{\boldsymbol{zz}}(k) = \boldsymbol{H}(k)\overline{\boldsymbol{C}}\,\boldsymbol{R}_{\boldsymbol{bb}}[\boldsymbol{H}(k)\overline{\boldsymbol{C}}]^{\rm H} + \sigma_v^2\boldsymbol{I}_{N(L_{\rm e}+1)} \tag{26}$$

$$\boldsymbol{R}_{\boldsymbol{zs}}(k) = \boldsymbol{H}(k)\overline{\boldsymbol{C}}\boldsymbol{R}_{\boldsymbol{bs}} \tag{27}$$

where the entries of $\boldsymbol{R}_{\boldsymbol{bb}} \triangleq \mathbb{E}[\boldsymbol{b}(k)\,\boldsymbol{b}^{\rm H}(k)] \in \mathbb{C}^{(QL_{\rm a}+L_{\rm c})\times(QL_{\rm a}+L_{\rm c})}$, as well as those of $\boldsymbol{R}_{\boldsymbol{bs}} \triangleq \mathbb{E}[\boldsymbol{b}(k)\boldsymbol{s}^{\rm H}(k-d)] \in \mathbb{C}^{(QL_{\rm a}+L_{\rm c})\times Q}$, do not depend on k and can be calculated by using the known correlation properties of the pseudo-symbols [22], [30].

B. FIRST STAGE: WLTV CHANNEL EQUALIZATION

It can be shown [30] that, for $h = 1/2 + k$, with $k \in \mathbb{Z}$, one-sided CPM signals are *noncircular* or *improper* (see [20], [21]). In this case, it is well known (see [21], [31]–[38]) that *widely-linear* signal processing techniques, which jointly elaborate the received signal and its complex conjugate version, allow to improve the performance.

The input-output relationship of a causal FIR WLTV equalizer of order $L_{\rm e} > 0$ is given by

$$\boldsymbol{y}(k) = \boldsymbol{F}_1^{\rm H}(k)\boldsymbol{z}(k) + \boldsymbol{F}_2^{\rm H}(k)\boldsymbol{z}^*(k) = \widetilde{\boldsymbol{F}}^{\rm H}(k)\tilde{\boldsymbol{z}}(k) \tag{28}$$

[2] Due to the time-varying assumption for the channel, the matrix $\boldsymbol{H}(k)$ loses its typical Toeplitz structure.

This article has been accepted for publication in a future issue of this journal, but has not been fully edited. Content may change prior to final publication. Citation information: DOI 10.1109/ACCESS.2018.2791098, IEEE Access

$$\boldsymbol{H}(k) \triangleq \begin{bmatrix} \boldsymbol{H}_0(k) & \boldsymbol{H}_1(k) & \dots & \boldsymbol{H}_{L_\mathrm{h}}(k) & \boldsymbol{O}_{N\times N} & \dots & \boldsymbol{O}_{N\times N} \\ \boldsymbol{O}_{N\times N} & \boldsymbol{H}_0(k-1) & \boldsymbol{H}_1(k-1) & \dots & \boldsymbol{H}_{L_\mathrm{h}}(k-1) & \ddots & \boldsymbol{O}_{N\times N} \\ \vdots & \ddots & \ddots & \ddots & \ddots & \ddots & \vdots \\ \boldsymbol{O}_{N\times N} & \dots & \ddots & \boldsymbol{H}_0(k-L_\mathrm{e}) & \boldsymbol{H}_1(k-L_\mathrm{e}) & \dots & \boldsymbol{H}_{L_\mathrm{h}}(k-L_\mathrm{e}) \end{bmatrix} \tag{15}$$

$$\boldsymbol{E}_d \triangleq \begin{bmatrix} \boldsymbol{e}_{d,0} & \boldsymbol{0}_{L_0+L_\mathrm{a}} & \cdots & \boldsymbol{0}_{L_0+L_\mathrm{a}} & \boldsymbol{0}_{L_0+L_\mathrm{a}} \\ \boldsymbol{0}_{L_1+L_\mathrm{a}} & \boldsymbol{e}_{d,1} & \cdots & \boldsymbol{0}_{L_1+L_\mathrm{a}} & \boldsymbol{0}_{L_1+L_\mathrm{a}} \\ \vdots & \vdots & \ddots & \vdots & \vdots \\ \boldsymbol{0}_{L_{Q-2}+L_\mathrm{a}} & \boldsymbol{0}_{L_{Q-2}+L_\mathrm{a}} & \cdots & \boldsymbol{e}_{d,Q-2} & \boldsymbol{0}_{L_{Q-2}+L_\mathrm{a}} \\ \boldsymbol{0}_{L_{Q-1}+L_\mathrm{a}} & \boldsymbol{0}_{L_{Q-1}+L_\mathrm{a}} & \cdots & \boldsymbol{0}_{L_{Q-1}+L_\mathrm{a}} & \boldsymbol{e}_{d,Q-1} \end{bmatrix} \tag{20}$$

for $k \in \mathbb{Z}$, where $\boldsymbol{F}_1(k), \boldsymbol{F}_2(k) \in \mathbb{C}^{N(L_\mathrm{e}+1)\times Q}$ collect all of the equalizer parameters, $\widetilde{\boldsymbol{F}}(k) \triangleq [\widetilde{\boldsymbol{F}}_1^{\mathrm{T}}(k), \widetilde{\boldsymbol{F}}_2^{\mathrm{T}}(k)]^{\mathrm{T}} \in \mathbb{C}^{2N(L_\mathrm{e}+1)\times Q}$ and $\tilde{\boldsymbol{z}}(k) \triangleq [\boldsymbol{z}^{\mathrm{T}}(k), \boldsymbol{z}^{\mathrm{H}}(k)]^{\mathrm{T}} \in \mathbb{C}^{2N(L_\mathrm{e}+1)}$.

On the basis of (14), the vector $\tilde{\boldsymbol{z}}(k)$ can be expressed as

$$\tilde{\boldsymbol{z}}(k) = \widetilde{\boldsymbol{H}}(k)\widetilde{\boldsymbol{C}}\tilde{\boldsymbol{b}}(k) + \tilde{\boldsymbol{w}}(k) \tag{29}$$

where $\widetilde{\boldsymbol{H}}(k) \in \mathbb{C}^{2N(L_\mathrm{e}+1)\times 2N(L_\mathrm{a}+1)}$ is the *augmented* channel matrix, defined as

$$\widetilde{\boldsymbol{H}}(k) \triangleq \begin{bmatrix} \boldsymbol{H}(k) & \boldsymbol{O}_{N(L_\mathrm{e}+1)\times N(L_\mathrm{a}+1)} \\ \boldsymbol{O}_{N(L_\mathrm{e}+1)\times N(L_\mathrm{a}+1)} & \boldsymbol{H}^*(k) \end{bmatrix} \tag{30}$$

whereas

$$\widetilde{\boldsymbol{C}} \triangleq \boldsymbol{I}_2 \otimes \overline{\boldsymbol{C}} \in \mathbb{R}^{2N(L_\mathrm{a}+1)\times 2(QL_\mathrm{a}+L_\mathrm{c})} \tag{31}$$

$$\tilde{\boldsymbol{b}}(k) \triangleq [\boldsymbol{b}^{\mathrm{T}}(k), \boldsymbol{b}^{\mathrm{H}}(k)]^{\mathrm{T}} \in \mathbb{C}^{2(QL_\mathrm{a}+L_\mathrm{c})} \tag{32}$$

$$\tilde{\boldsymbol{w}}(k) \triangleq [\boldsymbol{w}^{\mathrm{T}}(k), \boldsymbol{w}^{\mathrm{H}}(k)]^{\mathrm{T}} \in \mathbb{C}^{2N(L_\mathrm{e}+1)}\,. \tag{33}$$

It can be proven [30] that, for $h = 1/2 + k$, with $k \in \mathbb{Z}$, the pseudo-symbols (3) are related to their complex conjugates by the relationship

$$s^*_{q,n} = (-1)^{n+1+N_q^{(1)}} s_{q,n} \tag{34}$$

$\forall n \in \mathbb{N}_0$, where $N_q^{(1)} \triangleq \sum_{\ell=0}^{L-1} \beta_{q,\ell}$, with $q \in \{0, 1, \dots, Q-1\}$. Therefore, on the basis of (34), we can express the conjugate vector $\boldsymbol{b}^*(k)$ as follows

$$\boldsymbol{b}^*(k) = (-1)^{k+1}\widetilde{\boldsymbol{J}}\boldsymbol{b}(k) \tag{35}$$

where $\widetilde{\boldsymbol{J}} \in \mathbb{Z}^{(QL_\mathrm{a}+L_\mathrm{c})\times(QL_\mathrm{a}+L_\mathrm{c})}$ is a block diagonal matrix such that $\{\widetilde{\boldsymbol{J}}\}_{q,q} = (-1)^{N_q^{(1)}}\boldsymbol{J}_{L_\mathrm{a}+L_q}$, with $q \in \{0, 1, \dots, Q-1\}$. In this way, eq. (29) can be rewritten as

$$\tilde{\boldsymbol{z}}(k) = \widetilde{\boldsymbol{H}}(k)\widetilde{\boldsymbol{C}}\begin{bmatrix} \boldsymbol{I}_{QL_\mathrm{a}+L_\mathrm{c}} \\ (-1)^{k+1}\widetilde{\boldsymbol{J}} \end{bmatrix}\boldsymbol{b}(k) + \tilde{\boldsymbol{w}}(k)\,. \tag{36}$$

To simplify the previous model, we resort to the *derotation* approach [39], which consists of multiplying the vector $\boldsymbol{z}^*(k)$ by the alternating signal $(-1)^{k+1}$, with $k \in \mathbb{Z}$, and then applying the WLTV equalization to the modified input vector, thus yielding

$$\tilde{\boldsymbol{z}}_\mathrm{d}(k) \triangleq \begin{bmatrix} \boldsymbol{z}(k) \\ (-1)^{k+1}\boldsymbol{z}^*(k) \end{bmatrix} = \widetilde{\boldsymbol{H}}(k)\widetilde{\boldsymbol{C}}\widetilde{\boldsymbol{D}}\boldsymbol{b}(k) + \tilde{\boldsymbol{w}}_\mathrm{d}(k) \tag{37}$$

where

$$\widetilde{\boldsymbol{D}} \triangleq [\boldsymbol{I}_{QL_\mathrm{a}+L_\mathrm{c}}, \widetilde{\boldsymbol{J}}]^{\mathrm{T}} \in \mathbb{Z}^{2(QL_\mathrm{a}+L_\mathrm{c})\times(QL_\mathrm{a}+L_\mathrm{c})} \tag{38}$$

$$\tilde{\boldsymbol{w}}_\mathrm{d}(k) \triangleq [\boldsymbol{w}^{\mathrm{T}}(k), (-1)^{k+1}\boldsymbol{w}^{\mathrm{H}}(k)]^{\mathrm{T}}\,. \tag{39}$$

In the forthcoming two subsections, the WL versions of the ZF and MMSE equalizers are derived.

1) WLTV-ZF equalizer

The synthesis of the WLTV equalizer is similar in principle to that of the LTV one. Setting $\tilde{\boldsymbol{z}}(k) = \tilde{\boldsymbol{z}}_\mathrm{d}(k)$ in (28), the ZF condition $\boldsymbol{y}(k) = \boldsymbol{s}(k-d)$ leads to

$$\widetilde{\boldsymbol{F}}^{\mathrm{H}}(k)\widetilde{\boldsymbol{H}}(k)\widetilde{\boldsymbol{C}}\widetilde{\boldsymbol{D}} = \boldsymbol{E}_d^{\mathrm{T}} \tag{40}$$

whose minimal norm solution is given by

$$\widetilde{\boldsymbol{F}}_{\mathrm{ZF}}(k) = \widetilde{\boldsymbol{H}}(k)\widetilde{\boldsymbol{C}}\widetilde{\boldsymbol{D}}[\widetilde{\boldsymbol{D}}^{\mathrm{T}}\widetilde{\boldsymbol{C}}^{\mathrm{T}}\widetilde{\boldsymbol{H}}^{\mathrm{H}}(k)\widetilde{\boldsymbol{H}}(k)\widetilde{\boldsymbol{C}}\widetilde{\boldsymbol{D}}]^{-1}\boldsymbol{E}_d\,. \tag{41}$$

The condition $\mathrm{rank}[\widetilde{\boldsymbol{H}}(k)\widetilde{\boldsymbol{C}}\widetilde{\boldsymbol{D}}] = QL_\mathrm{a} + L_\mathrm{c}$, $\forall k \in \mathbb{Z}$, assures the consistency of the system in (40) and, thus, the existence of the WLTV-ZF equalizer. A necessary condition to ensure consistency is that $QL_\mathrm{a} + L_\mathrm{c} = Q(L_\mathrm{e} + L_\mathrm{h}) + L_\mathrm{c} \leq 2N(L_\mathrm{e}+1)$, from which

$$L_\mathrm{e} \geq \frac{QL_\mathrm{h} + L_\mathrm{c} - 2N}{2N - Q}\,. \tag{42}$$

Compared to (23), the consistency condition (42) might be satisfied for a full response CPM ($Q = 1$) with a finite L_e even when there is no oversampling ($N = 1$).

2) WLTV-MMSE equalizer

A WL version of the MMSE equalizer can be synthesized by minimizing the cost function

$$\mathrm{MSE}[\widetilde{\boldsymbol{F}}(k)] \triangleq \mathbb{E}[\|\boldsymbol{y}(k) - \boldsymbol{s}(k-d)\|^2] \tag{43}$$

for all $k \in \mathbb{Z}$, where $\boldsymbol{y}(k)$ is given by (28) and $\tilde{\boldsymbol{z}}(k) = \tilde{\boldsymbol{z}}_\mathrm{d}(k)$. In this case, the solution is given [29] by

$$\widetilde{\boldsymbol{F}}_{\mathrm{MMSE}}(k) = \boldsymbol{R}^{-1}_{\tilde{\boldsymbol{z}}_\mathrm{d}\tilde{\boldsymbol{z}}_\mathrm{d}}(k)\boldsymbol{R}_{\tilde{\boldsymbol{z}}_\mathrm{d}\boldsymbol{s}}(k) \tag{44}$$

This article has been accepted for publication in a future issue of this journal, but has not been fully edited. Content may change prior to final publication. Citation information: DOI 10.1109/ACCESS.2018.2791098, IEEE Access

where $\boldsymbol{R}_{\tilde{\mathbf{z}}_\mathrm{d}\tilde{\mathbf{z}}_\mathrm{d}}(k) \triangleq \mathbb{E}[\tilde{\mathbf{z}}_\mathrm{d}(k)\tilde{\mathbf{z}}_\mathrm{d}^\mathrm{H}(k)] \in \mathbb{C}^{2N(L_\mathrm{e}+1)\times 2N(L_\mathrm{e}+1)}$ and $\boldsymbol{R}_{\tilde{\mathbf{z}}_\mathrm{d}\boldsymbol{s}}(k) \triangleq \mathbb{E}[\tilde{\mathbf{z}}_\mathrm{d}(k)\boldsymbol{s}^\mathrm{H}(k-d)] \in \mathbb{C}^{2N(L_\mathrm{e}+1)\times Q}$. From (37) and assumptions **(a2)**–**(a3)**, one has

$$\boldsymbol{R}_{\tilde{\mathbf{z}}_\mathrm{d}\tilde{\mathbf{z}}_\mathrm{d}}(k) = \widetilde{\boldsymbol{H}}(k)\widetilde{\boldsymbol{C}}\widetilde{\boldsymbol{D}}\boldsymbol{R}_{\boldsymbol{bb}}[\widetilde{\boldsymbol{H}}(k)\widetilde{\boldsymbol{C}}\widetilde{\boldsymbol{D}}]^\mathrm{H} + \sigma_v^2\boldsymbol{I}_{2N(L_\mathrm{e}+1)} \tag{45}$$

$$\boldsymbol{R}_{\tilde{\mathbf{z}}_\mathrm{d}\boldsymbol{s}}(k) = \widetilde{\boldsymbol{H}}(k)\widetilde{\boldsymbol{C}}\widetilde{\boldsymbol{D}}\boldsymbol{R}_{\boldsymbol{bs}}\,. \tag{46}$$

C. SECOND STAGE: CPM SYMBOL DETECTION

The second stage processes the pseudo-symbol estimates at the output of the first stage to recover the transmitted binary sequence $\{a_n\}_{n\geq 0}$. Based on (3), the generic qth pseudo-symbol in the interval $t \in [kT,(k+1)T]$, with $k \geq L$, can be expressed as

$$\begin{aligned} s_{q,k} &= s_{0,k-L}\exp(j\pi h a_k)\prod_{\ell=1}^{L-1}\exp[j\pi h(1-\beta_{q,\ell})a_{k-\ell}] \\ &= s_{0,k-L}\exp(j\pi h a_k)\prod_{\ell=1}^{L-1}(s_{0,k-\ell}s_{0,k-\ell-1}^*)^{1-\beta_{q,\ell}} \end{aligned} \tag{47}$$

from which one obtains

$$\boldsymbol{s}(k) = \exp(j\pi h a_k)\boldsymbol{\rho}(k) \tag{48}$$

where $\boldsymbol{\rho}(k) \triangleq [\rho_0[\boldsymbol{a}_s(k)],\rho_1[\boldsymbol{a}_s(k)],\ldots,\rho_{Q-1}[\boldsymbol{a}_s(k)]]^\mathrm{T} \in \mathbb{C}^Q$, with

$$\rho_q[\boldsymbol{a}_s(k)] \triangleq s_{0,k-L}\prod_{\ell=1}^{L-1}\exp[j\pi h(1-\beta_{q,\ell})a_{k-\ell}] \tag{49}$$

and $\boldsymbol{a}_s(k) \triangleq [a_{k-1},a_{k-2},\ldots,a_{k-L+1}]^\mathrm{T} \in \{-1,1\}^{L-1}$. It is clear from (47) that, in general, the pseudo-symbol $s_{q,k}$, with $q \in \{0,1,\ldots,Q-1\}$ and $k \in \mathbb{Z}$, depends on the pseudo-symbol $s_{0,k-L}$ and the last $L-1$ symbols $\{a_{k-1},a_{k-2},\ldots,a_{k-L+1}\}$, as well as the symbol a_k. Let $\boldsymbol{y}(k)$ be the output of the equalizer, this suggests that one can use the VA, albeit in the presence of colored noise, to extract an estimate $\hat{a}_{k-d}$ of a_{k-d} from each entry of $\boldsymbol{y}(k) \approx \boldsymbol{s}(k-d)$, for high signal-to-noise ratio (SNR). In the following section, we propose suboptimal yet computationally efficient recursive strategies to this end.

IV. LOW-COMPLEXITY IMPLEMENTATION

The LTV or WLTV designs are considerably less computationally demanding than ML detection, even when the latter is based on VA. Nevertheless, properties of Laurent decomposition, as well as a careful analysis of the nonlinear mapping between symbols and pseudosymbols, allow for further simplifications of the two-stage proposed receiver.

A. SIMPLIFICATION OF THE FIRST STAGE

The number of PAM components involved in Laurent representation [22] increases exponentially with the length L of the frequency response. However, the same representation can be used to synthesize simplified versions of both LTV and WLTV equalizers. The key to achieve such a complexity reduction is to *approximate* the CPM signal by a sum of $Q_\mathrm{t} < Q = 2^{L-1}$ PAM components, such that to recover only a subset of $Q_\mathrm{r} \leq Q_\mathrm{t}$ corresponding pseudo-symbols, where Q_r and Q_t are design parameters. This represents a viable strategy because it is well known that the first Laurent pulse $c_{\mathrm{a},0}(t)$ is not only the longest one, but it also contains most of the energy [22]. Such a feature is manifest when particular frequency shape pulses and modulation indices are used [26]. Moreover, the fact that higher-order Laurent pulses have low energy negatively affects the rank of $\overline{\boldsymbol{C}}$ in (14), making the problem inherently ill-conditioned. Thus, discarding the contribution of higher-order pulses is also a useful strategy to obtain a robust solution.

In our models, the complexity reduction can be simply obtained by substituting Q with $Q_\mathrm{t} < Q$ in (14), and following the same derivations for all the synthesized equalizers. When a truncated Laurent representation is used, and a reduced number of pseudo-symbols are recovered, the dimensions of some matrices must be properly changed, i.e.,

$$\boldsymbol{E}_d, \boldsymbol{R}_{\boldsymbol{bs}} \in \mathbb{C}^{(Q_\mathrm{t}L_\mathrm{a}+\tilde{L}_\mathrm{c})\times Q_\mathrm{r}} \tag{50}$$

$$\overline{\boldsymbol{C}} \in \mathbb{R}^{N(L_\mathrm{a}+1)\times(Q_\mathrm{t}L_\mathrm{a}+\tilde{L}_\mathrm{c})} \tag{51}$$

$$\widetilde{\boldsymbol{D}} \in \mathbb{Z}^{2(Q_\mathrm{t}L_\mathrm{a}+\tilde{L}_\mathrm{c})\times(Q_\mathrm{t}L_\mathrm{a}+\tilde{L}_\mathrm{c})} \tag{52}$$

with $\tilde{L}_\mathrm{c} \triangleq \sum_{q=0}^{Q_\mathrm{t}-1} L_q$. Moreover, the necessary conditions for the existence of the ZF equalizers boil down to

$$L_\mathrm{e} \geq \frac{Q_\mathrm{t}L_\mathrm{h}+\tilde{L}_\mathrm{c}-N}{N-Q_\mathrm{t}} \tag{53}$$

$$L_\mathrm{e} \geq \frac{Q_\mathrm{t}L_\mathrm{h}+\tilde{L}_\mathrm{c}-2N}{2N-Q_\mathrm{t}} \tag{54}$$

for the LTV-ZF and WLTV-ZF case, respectively. The requirement on the length L_e of the equalizer is relaxed in both the linear and WL cases.

B. SIMPLIFICATION OF THE SECOND STAGE

Let the modulation index $h = m/p$, with $m,p \in \mathbb{Z}$. In this case the number of states to be considered in the VA aimed at recovering symbols form pseudo-symbols would be $p2^{L-1}$ if m is even, otherwise $p2^L$ if m is odd. For instance, if $L = 3$ and $h = 0.7$, we could have 80 states. In such a case, employing the VA in the second stage is not a viable strategy, due to the huge number of trellis states.

Hereinafter, we propose to resort to a simple least-squares (LS) estimator of a_k. Indeed, considering (48), we minimize the cost function $\|\boldsymbol{s}(k-d)-\boldsymbol{y}(k)\|^2$ with respect to a_{k-d}. The solution is obtained with straightforward calculations:

$$\hat{a}_{k-d} = \frac{1}{\pi h}\arg\{\boldsymbol{\rho}^\mathrm{H}(k-d)\boldsymbol{y}(k)\}\,. \tag{55}$$

Further simplifications can be obtained by employing only the first Q_r pseudo-symbols for symbol recovery, in which case $\boldsymbol{\rho}(k-d)$ and $\boldsymbol{y}(k)$ must be replaced by Q_r-length vectors. In the simplest case $Q_\mathrm{r} = 1$, eq. (55) can be rewritten as

$$\hat{a}_{k-d} = \frac{1}{\pi h}\arg\{y(k)\,y^*(k-1)\}\,. \tag{56}$$

It is worth noticing that, when $h = 0.5$, one has

$$s_{0,k} = s_{0,k-1}\exp\left(j\frac{\pi}{2}a_k\right) = ja_k\,s_{0,k-1} \tag{57}$$

This article has been accepted for publication in a future issue of this journal, but has not been fully edited. Content may change prior to final publication. Citation information: DOI 10.1109/ACCESS.2018.2791098, IEEE Access

from which it can be inferred that (56) can also be written as

$$\hat{a}_{k-d} = \Im\{y(k)y^*(k-1)\} \tag{58}$$

which is a common recursive detection rule for GMSK signals [26].

V. CHANNEL BEM AND FRESH REPRESENTATION

The synthesis of the first stage in Section III has been carried out without assuming a particular model for the LTV channel. In this section, we exploit the parsimonious CE-BEM representation [11], [15], [40] of the LTV channel to obtain alternative forms of the receivers in the frequency domain, so called FRESH representations [23].

The starting point is to express the discrete-time CIR $h(k,\ell)$ in (6) via the CE-BEM as

$$h(k,\ell) = \sum_{q=-Q_h/2}^{Q_h/2} h_q(\ell) \exp\left(j\frac{2\pi}{P}qk\right) \tag{59}$$

with $k \in \mathscr{K}$ and $\ell \in \{0,1,\ldots,NL_{\rm h}\}$, where

$$\mathscr{K} \triangleq \{k_0N, k_0N+1, \ldots, k_0N+N-1, (k_0+1)N, (k_0+1)N+1, \ldots, k_0N+KN-1\} \tag{60}$$

is the observation window of finite length $K > 1$ (expressed in symbols), with $k_0 \in \mathbb{Z}$, $L_{\rm h}$ is the channel length (expressed in symbols), $P \geq KN$, $Q_h \triangleq \lceil 2f_{\max}PT_{\rm c}\rceil$, and $f_{\max}$ denotes the Doppler spread of the channel.

When the CE-BEM is *oversampled*, i.e., $P > KN$, model (59) ensures a better level of accuracy in approximating many wireless channels. Hereinafter, we assume that: **(a5)** the coefficients $\{h_q(\ell)\}_{q=-Q_h/2}^{Q_h/2}$ are perfectly known at the receiver, $\forall \ell \in \{0,1,\ldots,NL_{\rm h}\}$; they can be estimated blindly [11], [18], [19] or by means of training sequences [41], [42].

By employing the CE-BEM (59), matrix $\boldsymbol{H}(k)$ in (14) can be similarly expanded as

$$\boldsymbol{H}(k) = \sum_{q=-Q_h/2}^{Q_h/2} \boldsymbol{H}_q \exp\left(j\frac{2\pi}{P}qkN\right) \tag{61}$$

where $\boldsymbol{H}_q \triangleq (\boldsymbol{W}_q \otimes \boldsymbol{I}_N)\overline{\boldsymbol{H}}_q \in \mathbb{C}^{N(L_{\rm e}+1)\times N(L_{\rm a}+1)}$, with $\boldsymbol{W}_q$ a diagonal matrix whose $(i+1,i+1)$th element is given by $\{\boldsymbol{W}_q\}_{ii} = \exp(-j\frac{2\pi}{P}qiN)$, with $i \in \{0,1,\ldots,L_{\rm e}\}$, and $\overline{\boldsymbol{H}}_q \in \mathbb{C}^{N(L_{\rm e}+1)\times N(L_{\rm a}+1)}$ is an upper-triangular block Toeplitz matrix, whose first N rows are given by $[\boldsymbol{H}_{0,q}, \boldsymbol{H}_{1,q}, \ldots, \boldsymbol{H}_{L_{\rm h},q}, \boldsymbol{O}_{N\times N}, \ldots, \boldsymbol{O}_{N\times N}]$, with

$$\{\boldsymbol{H}_{\ell,q}\}_{i_1,i_2} = h_q(\ell N + i_1 - i_2)\exp\left(j\frac{2\pi}{P}qi_1\right) \tag{62}$$

$\forall i_1, i_2 \in \{0,1,\ldots,N-1\}$. Letting $R \triangleq P/N$ (assumed to be integer), matrices $\boldsymbol{H}(k)$ and $\widetilde{\boldsymbol{H}}(k)$ can be equivalently rewritten as

$$\boldsymbol{H}(k) = \sum_{p=0}^{R-1} \boldsymbol{H}^{[p]} \exp\left(j\frac{2\pi}{R}pk\right) \tag{63}$$

$$\widetilde{\boldsymbol{H}}(k) = \sum_{p=0}^{R-1} \widetilde{\boldsymbol{H}}^{[p]} \exp\left(j\frac{2\pi}{R}pk\right) \tag{64}$$

where

$$\boldsymbol{H}^{[p]} \triangleq \begin{cases} \boldsymbol{H}_p, & 0 \leq p \leq Q_h/2\,; \\ \boldsymbol{O}_{N(L_{\rm e}+1)\times N(L_{\rm a}+1)}, & Q_h/2+1 \leq p \leq R-Q_h/2-1\,; \\ \boldsymbol{H}_{p-R}, & R-Q_h/2 \leq p \leq R-1\,. \end{cases} \tag{65}$$

and

$$\widetilde{\boldsymbol{H}}^{[p]} \triangleq \begin{bmatrix} \boldsymbol{H}^{[p]} & \boldsymbol{O}_{N(L_{\rm e}+1)\times N(L_{\rm a}+1)} \\ \boldsymbol{O}_{N(L_{\rm e}+1)\times N(L_{\rm a}+1)} & \boldsymbol{H}^{[(-p)_R]*} \end{bmatrix}. \tag{66}$$

It should be noted that (63) and (64) are the discrete Fourier series (DFS) expansions, with period R, of the periodically time-varying matrices $\boldsymbol{H}(k)$ and $\widetilde{\boldsymbol{H}}(k)$, respectively, with $\boldsymbol{H}^{[p]}$ and $\widetilde{\boldsymbol{H}}^{[p]}$ representing the DFS coefficients. As a consequence, the LTV and WLTV equalizers turn out to be periodic with the same period R and, thus, they can be expressed by means of their DFS representation over R points:

$$\boldsymbol{F}(k) = \sum_{p=0}^{R-1} \boldsymbol{F}^{[p]} \exp\left(j\frac{2\pi}{R}pk\right) \tag{67}$$

$$\widetilde{\boldsymbol{F}}(k) = \sum_{p=0}^{R-1} \widetilde{\boldsymbol{F}}^{[p]} \exp\left(j\frac{2\pi}{R}pk\right) \tag{68}$$

where $\boldsymbol{F}^{[p]} \in \mathbb{C}^{N(L_{\rm e}+1)\times Q}$ and $\widetilde{\boldsymbol{F}}^{[p]} \in \mathbb{C}^{2N(L_{\rm e}+1)\times Q}$ are the DFS coefficients of the LTV and WLTV equalizer matrices, respectively. In the following, we directly obtain the expressions of $\boldsymbol{F}^{[p]}$ and $\widetilde{\boldsymbol{F}}^{[p]}$ for the ZF and MMSE design strategies.

1) FRESH LTV-ZF equalizer

Let $\boldsymbol{\Psi} \triangleq [\boldsymbol{F}^{[0]{\rm T}}, \boldsymbol{F}^{[1]{\rm T}}, \ldots, \boldsymbol{F}^{[R-1]{\rm T}}]^{\rm T} \in \mathbb{C}^{RN(L_{\rm e}+1)\times Q}$, by substituting (67) and (63), the ZF condition (19) is rewritten as

$$\overline{\boldsymbol{C}}_{\rm circ}{}^{\rm T}\boldsymbol{H}_{\rm circ}^{\rm H}\boldsymbol{\Psi} = \boldsymbol{E}_{\rm circ} \tag{69}$$

where $\overline{\boldsymbol{C}}_{\rm circ} \triangleq \boldsymbol{I}_R \otimes \overline{\boldsymbol{C}} \in \mathbb{R}^{RN(L_{\rm a}+1)\times R(QL_{\rm a}+L_{\rm c})}$, $\boldsymbol{H}_{\rm circ} \in \mathbb{C}^{RN(L_{\rm e}+1)\times RN(L_{\rm a}+1)}$ is a block circulant [43] matrix whose $(i+1,j+1)$th block, for $i,j \in \{0,1,\ldots,R-1\}$, is given by $\boldsymbol{H}^{[(i-j)_R]} \in \mathbb{C}^{N(L_{\rm e}+1)\times N(L_{\rm a}+1)}$, i.e.,

$$\boldsymbol{H}_{\rm circ} \triangleq \begin{bmatrix} \boldsymbol{H}^{[0]} & \boldsymbol{H}^{[R-1]} & \ldots & \boldsymbol{H}^{[2]} & \boldsymbol{H}^{[1]} \\ \boldsymbol{H}^{[1]} & \boldsymbol{H}^{[0]} & \ldots & \boldsymbol{H}^{[3]} & \boldsymbol{H}^{[3]} \\ \vdots & \vdots & \vdots & \vdots & \vdots \\ \boldsymbol{H}^{[R-1]} & \boldsymbol{H}^{[R-2]} & \ldots & \boldsymbol{H}^{[1]} & \boldsymbol{H}^{[0]} \end{bmatrix} \tag{70}$$

whereas $\boldsymbol{E}_{\rm circ} \triangleq [\boldsymbol{E}_d^{\rm T}, \boldsymbol{O}_{Q\times R(QL_{\rm a}+L_{\rm c})}]^{\rm T} \in \mathbb{B}^{R(QL_{\rm a}+L_{\rm c})\times Q}$.

Solution of (69), in the minimal-norm sense, is given by

$$\boldsymbol{\Psi}_{\rm ZF} = \boldsymbol{H}_{\rm circ}\overline{\boldsymbol{C}}_{\rm circ}\left(\overline{\boldsymbol{C}}_{\rm circ}{}^{\rm T}\boldsymbol{H}_{\rm circ}^{\rm H}\boldsymbol{H}_{\rm circ}\overline{\boldsymbol{C}}_{\rm circ}\right)^{-1}\boldsymbol{E}_{\rm circ}\,. \tag{71}$$

This article has been accepted for publication in a future issue of this journal, but has not been fully edited. Content may change prior to final publication. Citation information: DOI 10.1109/ACCESS.2018.2791098, IEEE Access

2) FRESH LTV-MMSE equalizer

The starting point for deriving the FRESH version of the LTV-MMSE solution is the system of linear equations

$$\boldsymbol{R}_{\boldsymbol{zz}}(k)\boldsymbol{F}(k) = \boldsymbol{R}_{\boldsymbol{zs}}(k)\,. \tag{72}$$

By taking into account (26) and (63), it can be proven that $\boldsymbol{R}_{\boldsymbol{zz}}(k)$ admits the DFS expansion

$$\boldsymbol{R}_{\boldsymbol{zz}}(k) = \sum_{p=0}^{R-1} \boldsymbol{R}_{\boldsymbol{zz}}^{[p]} \exp\left(j\frac{2\pi}{R}pk\right) \tag{73}$$

where the DFS coefficients $\{\boldsymbol{R}_{\boldsymbol{zz}}^{[p]}\}_{p=0}^{R-1} \in \mathbb{C}^{N(L_e+1)\times N(L_e+1)}$ are referred to as the *cyclic correlation matrices* [23] of $\boldsymbol{z}(k)$. By substituting (27), (63), (67), and (73) in (72), one obtains

$$\boldsymbol{R}_{\text{circ}}\boldsymbol{\Psi} = \boldsymbol{\Xi}\overline{\boldsymbol{C}}\boldsymbol{R}_{\boldsymbol{bs}} \tag{74}$$

where $\boldsymbol{\Xi} \triangleq \left[\boldsymbol{H}^{[0]\text{T}}, \boldsymbol{H}^{[1]\text{T}}, \ldots, \boldsymbol{H}^{[R-1]\text{T}}\right]^{\text{T}} \in \mathbb{C}^{RN(L_e+1)\times N(L_a+1)}$ and $\boldsymbol{R}_{\text{circ}} \in \mathbb{C}^{RN(L_e+1)\times RN(L_e+1)}$ is a block-circulant [43] matrix whose $(i+1,j+1)$th block, for $i,j \in \{0,1,\ldots,R-1\}$, is given by $\boldsymbol{R}_{\boldsymbol{zz}}^{[(i-j)_R]}$, i.e.,

$$\boldsymbol{R}_{\text{circ}} \triangleq \begin{bmatrix} \boldsymbol{R}_{\boldsymbol{zz}}^{[0]} & \boldsymbol{R}_{\boldsymbol{zz}}^{[R-1]} & \cdots & \boldsymbol{R}_{\boldsymbol{zz}}^{[2]} & \boldsymbol{R}_{\boldsymbol{zz}}^{[1]} \\ \boldsymbol{R}_{\boldsymbol{zz}}^{[1]} & \boldsymbol{R}_{\boldsymbol{zz}}^{[0]} & \cdots & \boldsymbol{R}_{\boldsymbol{zz}}^{[3]} & \boldsymbol{R}_{\boldsymbol{zz}}^{[2]} \\ \vdots & \vdots & \ddots & \vdots & \vdots \\ \boldsymbol{R}_{\boldsymbol{zz}}^{[R-1]} & \boldsymbol{R}_{\boldsymbol{zz}}^{[R-2]} & \cdots & \boldsymbol{R}_{\boldsymbol{zz}}^{[1]} & \boldsymbol{R}_{\boldsymbol{zz}}^{[0]} \end{bmatrix}. \tag{75}$$

The solution of (74) is given by

$$\boldsymbol{\Psi}_{\text{MMSE}} = \boldsymbol{R}_{\text{circ}}^{-1}\boldsymbol{\Xi}\overline{\boldsymbol{C}}\boldsymbol{R}_{\boldsymbol{bs}}\,. \tag{76}$$

3) FRESH WLTV-ZF equalizer

Considering the synthesis of the WLTV-ZF equalizer using the derotation approach, the equalizer represents the solution, in the minimal-norm sense, of the following linear system:

$$\widetilde{\boldsymbol{D}}^{\text{T}}\widetilde{\boldsymbol{C}}^{\text{T}}\widetilde{\boldsymbol{H}}^{\text{H}}(k)\widetilde{\boldsymbol{F}}(k) = \boldsymbol{E}_d\,. \tag{77}$$

Let $\widetilde{\boldsymbol{\Psi}} = [\widetilde{\boldsymbol{F}}^{[0]\text{T}}, \widetilde{\boldsymbol{F}}^{[1]\text{T}}, \ldots, \widetilde{\boldsymbol{F}}^{[R-1]\text{T}}] \in \mathbb{C}^{2RN(L_e+1)\times Q}$, by substituting (64) and (68), the ZF condition (77) is rewritten as

$$\widetilde{\boldsymbol{C}}_{\text{circ}}^{\text{T}}\widetilde{\boldsymbol{H}}_{\text{circ}}^{\text{H}}\widetilde{\boldsymbol{\Psi}} = \boldsymbol{E}_{\text{circ}} \tag{78}$$

where we defined $\widetilde{\boldsymbol{C}}_{\text{circ}} \triangleq \boldsymbol{I}_R \otimes (\widetilde{\boldsymbol{C}}\widetilde{\boldsymbol{D}}) \in \mathbb{R}^{2RN(L_a+1)\times R(QL_a+L_c)}$, and $\widetilde{\boldsymbol{H}}_{\text{circ}} \in \mathbb{C}^{2RN(L_e+1)\times 2RN(L_a+1)}$ is block circulant, whose $(i+1,j+1)$th block, for $i,j \in \{0,1,\ldots,R-1\}$, is given by $\widetilde{\boldsymbol{H}}^{[(i-j)_R]} \in \mathbb{C}^{2N(L_e+1)\times 2N(L_a+1)}$. The solution in the minimal-norm sense is given by

$$\widetilde{\boldsymbol{\Psi}}_{\text{ZF}} = \widetilde{\boldsymbol{H}}_{\text{circ}}\widetilde{\boldsymbol{C}}_{\text{circ}}(\widetilde{\boldsymbol{C}}_{\text{circ}}^{\text{T}}\widetilde{\boldsymbol{H}}_{\text{circ}}^{\text{H}}\widetilde{\boldsymbol{H}}_{\text{circ}}\widetilde{\boldsymbol{C}}_{\text{circ}})^{-1}\boldsymbol{E}_{\text{circ}}\,. \tag{79}$$

4) FRESH WLTV-MMSE equalizer

To derive the FRESH version of the WLTV-MMSE solution using the derotation approach, let us start from the following system of linear equations

$$\boldsymbol{R}_{\tilde{\boldsymbol{z}}_{\text{d}}\tilde{\boldsymbol{z}}_{\text{d}}}(k)\widetilde{\boldsymbol{F}}(k) = \boldsymbol{R}_{\tilde{\boldsymbol{z}}_{\text{d}}\boldsymbol{s}}(k)\,. \tag{80}$$

By taking into account (45) and (64), it can be proven that $\boldsymbol{R}_{\tilde{\boldsymbol{z}}_{\text{d}}\tilde{\boldsymbol{z}}_{\text{d}}}(k)$ admits the DFS expansion

$$\boldsymbol{R}_{\tilde{\boldsymbol{z}}_{\text{d}}\tilde{\boldsymbol{z}}_{\text{d}}}(k) = \sum_{p=0}^{R-1} \boldsymbol{R}_{\tilde{\boldsymbol{z}}_{\text{d}}\tilde{\boldsymbol{z}}_{\text{d}}}^{[p]} \exp\left(j\frac{2\pi}{R}pk\right) \tag{81}$$

where the DFS coefficients $\{\boldsymbol{R}_{\tilde{\boldsymbol{z}}_{\text{d}}\tilde{\boldsymbol{z}}_{\text{d}}}^{[p]}\}_{p=0}^{R-1} \in \mathbb{C}^{2N(L_e+1)\times 2N(L_e+1)}$ are referred to as the *cyclic correlation matrices* [23] of $\tilde{\boldsymbol{z}}_{\text{d}}(k)$. By substituting (46), (68), and (81) in (80), one obtains

$$\widetilde{\boldsymbol{R}}_{\text{circ}}\widetilde{\boldsymbol{\Psi}} = \widetilde{\boldsymbol{\Xi}}\widetilde{\boldsymbol{C}}\widetilde{\boldsymbol{D}}\boldsymbol{R}_{\boldsymbol{bs}} \tag{82}$$

where $\widetilde{\boldsymbol{\Xi}} \triangleq \left[\widetilde{\boldsymbol{H}}^{[0]\text{T}}, \widetilde{\boldsymbol{H}}^{[1]\text{T}}, \ldots, \widetilde{\boldsymbol{H}}^{[R-1]\text{T}}\right]^{\text{T}} \in \mathbb{C}^{RN(L_e+1)\times N(L_a+1)}$ and $\widetilde{\boldsymbol{R}}_{\text{circ}} \in \mathbb{C}^{2RN(L_e+1)\times 2RN(L_e+1)}$ is a block-circulant [43] matrix whose $(i+1,j+1)$th block, for $i,j \in \{0,1,\ldots,R-1\}$, is given by $\boldsymbol{R}_{\tilde{\boldsymbol{z}}_{\text{d}}\tilde{\boldsymbol{z}}_{\text{d}}}^{[(i-j)_R]}$. The solution of (82) is given by

$$\widetilde{\boldsymbol{\Psi}}_{\text{MMSE}} = \widetilde{\boldsymbol{R}}_{\text{circ}}^{-1}\widetilde{\boldsymbol{\Xi}}\widetilde{\boldsymbol{C}}\widetilde{\boldsymbol{D}}\boldsymbol{R}_{\boldsymbol{bs}}\,. \tag{83}$$

At this point, three remarks are in order.

Remark 1: Taking into account (67) and (68), the output of the FRESH-LTV and FRESH-WLTV equalizers can be written as $\boldsymbol{y}(k) = \boldsymbol{\Psi}^{\text{H}}[\boldsymbol{\zeta} \otimes \boldsymbol{z}(k)]$ and $\boldsymbol{y}(k) = \widetilde{\boldsymbol{\Psi}}^{\text{H}}[\boldsymbol{\zeta} \otimes \tilde{\boldsymbol{z}}_{\text{d}}(k)]$, respectively, where the $(i+1)$th element of $\boldsymbol{\zeta}(k) \in \mathbb{C}^R$ is $\zeta_i \triangleq \exp(-j\frac{2\pi}{R}ik)$, with $i \in \{0,1,\ldots,R-1\}$ and $k \in \mathbb{Z}$. That is, all the proposed time-varying equalizers can be regarded as a parallel bank of R LTI equalizers, each driven by a different frequency-shifted version of $\boldsymbol{z}(k)$ or $\tilde{\boldsymbol{z}}_{\text{d}}(k)$.

Remark 2: The FRESH solutions require inversion of large matrices [see (71), (76), (79), (83)]. However, reasoning as in [16], it can be shown that, due to the block circulant nature of such matrices, a much simpler inversion can be carried out operating on the smaller component blocks; moreover, the number of block inverses can be reduced by exploiting the Hermitian symmetry of the overall matrix.

Remark 3: Low-complexity versions of the FRESH receivers can be obtained as in [16] by truncating the DFS series of (67) and (68) to $Q_e+1 \ll R$ frequency shifts. The resulting FRESH implementation consists of a bank of only Q_e+1 LTI equalizers instead of R ones.

VI. NUMERICAL RESULTS

In this section, we present results of Monte Carlo computer simulations aimed at assessing the performance of the proposed LTV and WLTV equalizers, which are all implemented in their FRESH versions.

In all the experiments, the following common simulation setting was adopted. We considered a 200 Kbps CNPC link (symbol period $T = 5\ \mu$s) with carrier frequency $f_c = 5\,060$

This article has been accepted for publication in a future issue of this journal, but has not been fully edited. Content may change prior to final publication. Citation information: DOI 10.1109/ACCESS.2018.2791098, IEEE Access

Table 1. ABER for different (Q_t, Q_r) (GMSK with $L = 2$, $E_b/N_0 = 6$ dB).

Q_t	Q_r	LTV equalizers ZF	LTV equalizers MMSE	WLTV equalizers ZF	WLTV equalizers MMSE
1	1	**0.0819**	0.0400	**0.0048**	**0.0048**
2	1	0.4858	**0.0381**	0.1049	0.0048
	2	0.4860	0.0403	0.4783	0.0064

Table 2. ABER for different (Q_t, Q_r) (GMSK with $L = 3$, $E_b/N_0 = 6$ dB).

Q_t	Q_r	LTV equalizers ZF	LTV equalizers MMSE	WLTV equalizers ZF	WLTV equalizers MMSE
1	1	**0.2228**	0.0706	**0.0059**	0.0055
2	1	0.5014	**0.0705**	0.2964	0.0054
	2	0.5014	0.0793	0.4738	0.0104
3	1	0.5023	0.0714	0.3620	0.0062
	2	0.5023	0.0802	0.4734	0.0104
	3	0.5024	0.0803	0.5020	0.0104
4	1	0.4988	0.0715	0.4795	**0.0051**
	2	0.4988	0.0796	0.4874	0.0093
	3	0.4988	0.0796	0.4995	0.0094
	4	0.4988	0.0796	0.5006	0.0096

MHz (C-band), employing a binary GMSK modulation format (hence, $M = 2$ and $h = 1/2$) and operating over a doubly-selective wireless channel. We considered two different values of $L > 1$ (partial response CPM) for the GMSK modulation, i.e., $L \in \{2, 3\}$, corresponding to different pulse lengths, amount of memory, and bandwidth of the signal: in particular, the one-sided 99% energy bandwidth, evaluated by numerical methods, is approximately equal to 103 kHz for $L = 2$ and 94 kHz for $L = 3$.

The channel is modeled according to the *Arrival/Takeoff* Ricean channel model in [44], which exhibits a maximum delay spread of 7 μs; to better adapt it to the UAV scenario, we employed a Rice factor $K_{\text{rice}} = 29$ dB, which is typical [45] of hilly/mountainous scenarios. The UAV speed is equal to 90 m/s, corresponding to a maximum Doppler spread $f_{\max} = 1.52$ kHz and a channel coherence time of 0.66 ms.

The oversampling factor is $N = 8$, the discrete-time channel length in number of symbols is $L_h = 2$, the equalization delay d is chosen as the zero-based index of the column of $\overline{\boldsymbol{C}}$ given by (16) having maximal norm (note that this simple selection does not depend on the channel and can be conveniently performed off-line). The parameters of the oversampled BEM model are $K = 100$ (block size) and $P = 2KN = 1600$, resulting in $R = P/N = 2K = 200$ and $Q_h = \lceil 2 f_{\max} P T_c \rceil = 4$.

As performance measure, we adopted the average (over 10 channel realizations) bit-error rate (ABER), calculated for each channel realization over 10^6 data symbols. All the LTV and WLTV equalizers are implemented assuming perfect knowledge of the channel.[3]

Experiment 1: (ABER versus Q_t and Q_r). In the first set of simulations, for a fixed equalizer length $L_e + 1 = 4$ and energy contrast $E_b/N_0 = 6$ dB, we explored different design choices for (Q_t, Q_r), with $Q_r \le Q_t \le Q$, where $Q = 2^{L-1}$ is the number of Laurent pulses. In particular, it results that $Q = 2$ when $L = 2$ and, thus, only 3 different (Q_t, Q_r) configurations are allowed. On the other hand, we have $Q = 4$ for $L = 3$ and, hence, 10 different (Q_t, Q_r) configurations are considered. ABER results reported in Tab. 1 for $L = 2$ and Tab. 2 for $L = 3$ show that the optimal choice of the parameters (Q_t, Q_r) depends on the equalizer type (we marked in bold the best combinations for each equalizer type). The ZF versions of the equalizers are very sensitive to the choice of (Q_t, Q_r), exhibiting considerable degradations for $Q_t > 1$: this is due to severe ill-conditioning of the inversion problem, due to the addition of very small Laurent pulses. On the contrary, the performance of the MMSE versions of the equalizers is scarcely sensitive to the choice of (Q_t, Q_r). In general, for a given value of Q_t, the performance of both ZF and MMSE equalizers exhibits a monotonic degradation with increasing values of Q_r: it is thus advisable to rely only on the first pseudo-symbol to perform recursive symbol detection,[4] by setting $Q_r = 1$. In summary, since the overall design complexity increases with Q_t, it is preferable to choose the smallest values of Q_t and Q_r for all equalizers. For this reason, in the following experiments we set $Q_t = Q_r = 1$, which entails a very simple synthesis, based only on the first Laurent pulse.

Experiment 2 (ABER versus equalizer length). In the second simulation, we assessed the performance of the equalizer as a function of the equalizer length (in number of symbols) $L_e + 1$ ranging from 1 to 6, by setting $(Q_t, Q_r) = (1, 1)$ and $E_b/N_0 = 6$ dB. In Figs. 1 and 2, the ABER values are reported for $L = 2$ and $L = 3$, respectively. It is shown that the WLTV equalizers exhibit the best performance, with the WLTV-MMSE one providing good ABER values even with very small equalizer lengths. On the contrary, the performance of LTV equalizers is rather flat, exhibiting only a moderate improvement with L_e. A common trend for all equalizers is that increasing the equalizer length beyond $L_e + 1 = 4$, which is the minimum value satisfying $L_e \ge L_h + 1$, does not allow one to further improve the system performance, since the ABER curves tend to flatten out for larger values of L_e. Hence, selecting $L_e = L_h + 1$ is a good design choice, which is adopted in the following.

Experiment 3 (ABER versus E_b/N_0). In the third simulation, we explored the performance as a function of the signal level. In particular, in Figs. 3 and 4 we reported the ABER as a function of E_b/N_0 (in dB) ranging from 4 to 12, by choosing again $(Q_t, Q_r) = (1, 1)$ and, moreover, setting the equalizer length $L_e + 1 = 4$. Results of Figs. 3 and 4 show that the proposed equalizers, in particular the WLTV ones, can provide satisfactory performance for relatively small E_b/N_0 values. Consider that, in the same situations, VA-based ML detection optimized for the AWGN channel exhibits a marked BER floor at ABER values around to

[3] Nearly perfect channel estimation can be achieved if sufficiently long training sequences are employed [42].

[4] This behavior would call for the adoption of more sophisticated strategies, such as applying a weighted LS approach in the second stage, in order to properly weigh the different energies of the PAM components.

This article has been accepted for publication in a future issue of this journal, but has not been fully edited. Content may change prior to final publication. Citation information: DOI 10.1109/ACCESS.2018.2791098, IEEE Access

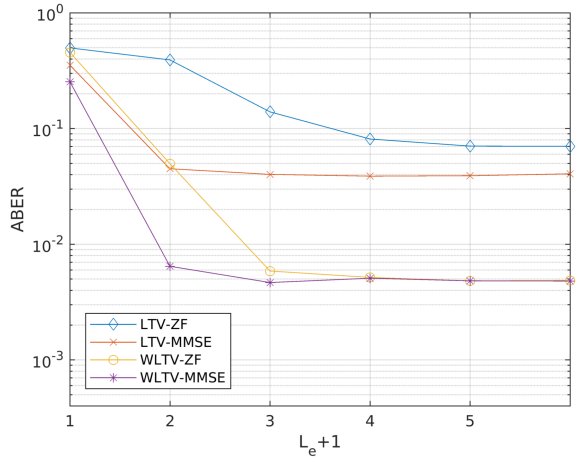

Figure 1. ABER vs. equalizer length L_e+1 (GMSK with $L=2$, $E_b/N_0=6$ dB).

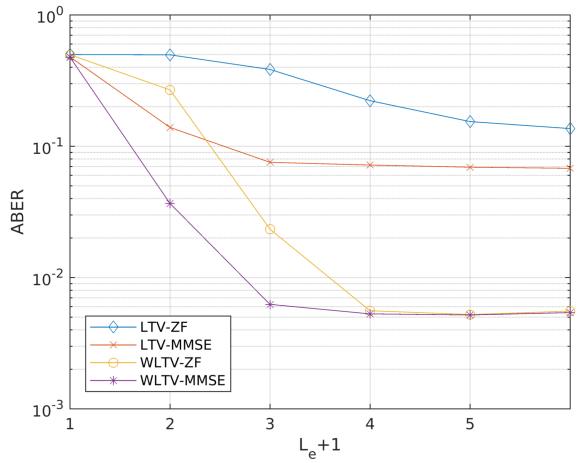

Figure 2. ABER vs. equalizer length L_e+1 (GMSK with $L=3$, $E_b/N_0=6$ dB).

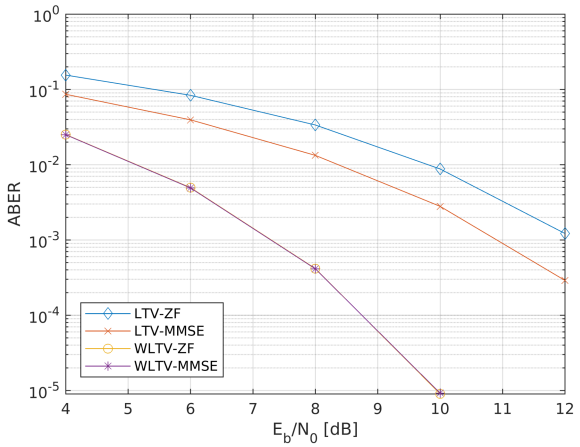

Figure 3. ABER vs. energy contrast E_b/N_0 (GMSK with $L=2$).

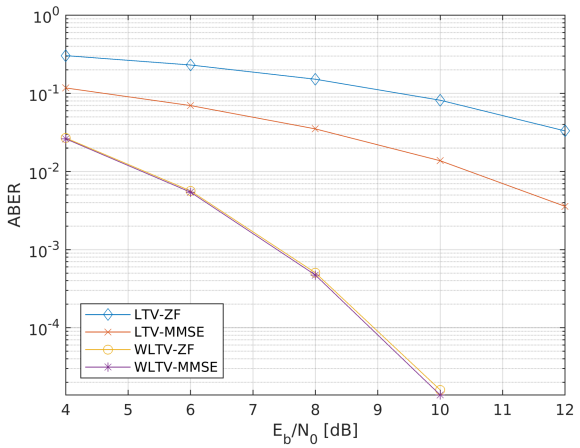

Figure 4. ABER vs. energy contrast E_b/N_0 (GMSK with $L=3$).

0.3. The performance is particularly good for the WLTV-ZF and WLTV-MMSE equalizers, which perform comparably, gaining approximately 4 dB over the LTV-MMSE at an ABER of 10^{-3} for $L=2$, and more than 5 dB for $L=3$ (in the latter case, we cannot precisely assess the E_b/N_0 gain, since a wider range of E_b/N_0 values for the LTV equalizers would be needed). It is worth noticing that the MMSE and ZF versions of the WLTV equalizer exhibit practically the same performance, whereas the LTV-MMSE equalizer performs consistently better than the LTV-ZF one. Finally, there is no significant difference in performance between the cases $L=2$ and $L=3$ for the WLTV equalizers, whereas the LTV ones perform better when $L=2$ compared to $L=3$.

VII. CONCLUSIONS

In this paper, we proposed new techniques for equalization of a UAV CNPC link operating over a doubly-selective wireless channel. By leveraging on the Laurent representation for a CPM signal and the BEM of the channel, and adopting the ZF or MMSE criteria, we synthesized both LTV and WLTV receivers, where the latter ones can be applied when the CPM signal, such as the GMSK one, is noncircular or improper. By exploiting the parameterization offered by both Laurent and BEM representations, we derived computationally-efficient versions of the proposed equalizers. Monte Carlo numerical simulations corroborate our design choice, and show that the proposed receiving structures provide good performances even for low-to-moderate values of energy contrast, in typical UAV scenarios.

References

[1] ITU-R M.2171, Characteristics of unmanned aircraft systems and spectrum requirements to support their safe operation in non-segregated airspace, International Telecommunication Union techreport, Dec. 2009.

[2] K. P. Valavanis and G. J. Vachtsevanos, Handbook of unmanned aerial vehicles, Springer, Ed. Springer, 2015.

[3] Y. Zeng, R. Zhang, and T. J. Lim, "Wireless communications with unmanned aerial vehicles: opportunities and challenges," IEEE Communications Magazine, vol. 54, no. 5, pp. 36–42, May 2016.

[4] Telemetry Group, Range Commander Council, "Telemetry Standards. IRIG Standard 106-04 Part I," Tech. Rep., May 2004. [Online]. Available: http://www.irig106.org/

[5] RTCA, Minimum operational performance standards (MOPS) for unmanned aircraft systems (UAS) command and control, RTCA Std., Rev. Ver 1.0, 2'15.
[6] J. B. Anderson, T. Aulin, and C. E. Sundberg, Digital Phase Modulation. Springer, 2013.
[7] J. G. Proakis, Digital communications, 4th ed. McGraw-Hill, 2000.
[8] J. Tan and G. L. Stuber, "Frequency-domain equalization for continuous phase modulation," IEEE Transactions on Wireless Communications, vol. 4, no. 5, pp. 2479–2490, 2005.
[9] F. Pancaldi and G. M. Vitetta, "Equalization algorithms in the frequency domain for continuous phase modulations," IEEE Transactions on Communications, vol. 54, no. 4, pp. 648–658, 2006.
[10] W. Van Thillo, F. Horlin, J. Nsenga, V. Ramon, A. Bourdoux, and R. Lauwereins, "Low-complexity linear frequency domain equalization for continuous phase modulation," IEEE Transactions on Wireless Communications, vol. 8, no. 3, pp. 1435–1445, 2009.
[11] G. B. Giannakis and C. Tepedelenlioglu, "Basis expansion models and diversity techniques for blind identification and equalization of time-varying channels," Proceedings of the IEEE, vol. 86, no. 10, pp. 1969–1986, 1998.
[12] X. Ma and G. B. Giannakis, "Maximum-diversity transmissions over doubly selective wireless channels," IEEE Transactions on Information Theory, vol. 49, no. 7, pp. 1832–1840, Jul. 2003.
[13] I. Barhumi, G. Leus, and M. Moonen, "Time-domain channel shortening and equalization of OFDM over doubly-selective channels," in Proc. and Signal Processing 2004 IEEE Int. Conf. Acoustics, Speech, vol. 3, May 2004, pp. iii–801–4 vol.3.
[14] J.-C. Chang, F.-B. Ueng, and J.-C. Ning, "Channel shortening and equalization of OFDM/CDMA systems over doubly selective fading channels," in International Symposium on Wireless and Pervasive Computing, Feb. 2011, pp. 1–4.
[15] I. Barhumi, G. Leus, and M. Moonen, "Time-varying FIR equalization for doubly selective channels," IEEE Transactions on Wireless Communications, vol. 4, no. 1, pp. 202–214, 2005.
[16] F. Verde, "Frequency-shift zero-forcing time-varying equalization for doubly selective SIMO channels," EURASIP Journal on Advances in Signal Processing, vol. 2006, no. 1, pp. 1–14, 2006.
[17] H. Kim and J. K. Tugnait, "Turbo equalization for doubly-selective fading channels using nonlinear kalman filtering and basis expansion models," IEEE Transactions on Wireless Communications, vol. 9, no. 6, pp. 2076–2087, June 2010.
[18] J. K. Tugnait and W. Luo, "Linear prediction error method for blind identification of periodically time-varying channels," IEEE Transactions on Signal Processing, vol. 50, no. 12, pp. 3070–3082, Dec. 2002.
[19] ——, "Blind identification of time-varying channels using multistep linear predictors," IEEE Transactions on Signal Processing, vol. 52, no. 6, pp. 1739–1749, 2004.
[20] F. D. Neeser and J. L. Massey, "Proper complex random processes with applications to information theory," IEEE Transactions on Information Theory, vol. 39, no. 4, pp. 1293–1302, Jul. 1993.
[21] B. Picinbono and P. Chevalier, "Widely linear estimation with complex data," IEEE Transactions on Signal Processing, vol. 43, no. 8, pp. 2030–2033, Aug. 1995.
[22] P. Laurent, "Exact and approximate construction of digital phase modulations by superposition of amplitude modulated pulses (AMP)," IEEE Transactions on Communications, vol. 34, no. 2, pp. 150–160, 1986.
[23] L. Franks, "Polyperiodic linear filtering," in Cyclostationarity in Communications and Signal Processing, W. A. Gardner, Ed. IEEE Press, 1994, pp. 240–266.
[24] A. Ben-Israel and T. N. E. Greville, Generalized Inverses: Theory and Applications. Springer, 2003.
[25] U. Mengali and M. Morelli, "Decomposition of M-ary CPM signals into PAM waveforms," IEEE Transactions on Information Theory, vol. 41, no. 5, pp. 1265–1275, 1995.
[26] G. K. Kaleh, "Simple coherent receivers for partial response continuous phase modulation," IEEE J. Sel. Areas Commun., vol. 7, no. 9, pp. 1427–1436, Dec. 1989.
[27] P. P. Vaidyanathan, Multirate systems and filter banks. Pearson Education India, 1993.
[28] M. A. Boujelben, F. Bellili, S. Affes, and A. Stephenne, "SNR estimation over SIMO channels from linearly modulated signals," IEEE Transactions on Signal Processing, vol. 58, no. 12, pp. 6017–6028, 2010.
[29] M. Honig, U. Madhow, and S. Verdu, "Blind adaptive multiuser detection," IEEE Transactions on Information Theory, vol. 41, no. 4, pp. 944–960, Jul. 1995.
[30] D. Darsena, G. Gelli, I. Iudice, and F. Verde, "Second-order statistics of one-sided CPM signals," IEEE Signal Processing Letters, vol. 24, no. 10, pp. 1512–1516, Oct. 2017.
[31] G. Gelli, L. Paura, and A. M. Tulino, "Cyclostationarity-based filtering for narrowband interference suppression in direct-sequence spread-spectrum systems," IEEE Journal on Selected Areas in Communications, vol. 16, no. 9, pp. 1747–1755, Dec. 1998.
[32] G. Gelli, L. Paura, and A. R. P. Ragozini, "Blind widely linear multiuser detection," IEEE Communications Letters, vol. 4, no. 6, pp. 187–189, Jun. 2000.
[33] H. Gerstacker, R. Schober, and A. Lampe, "Receivers with widely linear processing for frequency-selective channels," IEEE Transactions on Communications, vol. 51, no. 9, pp. 1512–1523, Sep. 2003.
[34] W. H. Gerstacker, F. Obernosterer, R. Schober, A. Lehmann, A. Lampe, and P. Gunreben, "Widely linear equalization for space-time block-coded transmission over fading ISI channels," in Proceedings IEEE 56th Vehicular Technology Conference, vol. 1, 2002, pp. 238–242 vol.1.
[35] A. Lampe, R. Schober, W. Gerstacker, and J. Huber, "A novel iterative multiuser detector for complex modulation schemes," IEEE Journal on Selected Areas in Communications, vol. 20, no. 2, pp. 339–350, Feb. 2002.
[36] Y. C. Yoon and H. Leib, "Maximizing SNR in improper complex noise and applications to CDMA," IEEE Communications Letters, vol. 1, no. 1, pp. 5–8, Jan. 1997.
[37] J.-J. Jeon, J. G. Andrews, and K.-M. Sung, "The blind widely linear minimum output energy algorithm for DS-CDMA systems," IEEE Transactions on Signal Processing, vol. 54, no. 5, pp. 1926–1931, May 2006.
[38] P. Chevalier and F. Pipon, "New insights into optimal widely linear array receivers for the demodulation of BPSK, MSK, and GMSK signals corrupted by noncircular interferences-application to SAIC," IEEE Transactions on Signal Processing, vol. 54, no. 3, pp. 870–883, Mar. 2006.
[39] Z. Ding and G. Li, "Single-channel blind equalization for GSM cellular systems," IEEE Journal on Selected Areas in Communications, vol. 16, no. 8, pp. 1493–1505, Oct. 1998.
[40] G. Leus, I. Barhumi, and M. Moonen, "Low-complexity serial equalization of doubly-selective channels," in Proceedings of Sixth Baiona Workshop on Signal Processing in Communications, 2003, pp. 69–74.
[41] X. Meng and J. K. Tugnait, "Semi-blind time-varying channel estimation using superimposed training," in Proceedings of IEEE International Conference on Acoustics, Speech, and Signal Processing (ICASSP '04), vol. 3, May 2004, pp. iii–797–800 vol.3.
[42] G. Leus, "On the estimation of rapidly time-varying channels," in Proceedings of 12th European Signal Processing Conference, 2004, pp. 2227–2230.
[43] R. A. Horn and C. R. Johnson, Matrix analysis. Cambridge University Press, 2012.
[44] E. Haas, "Aeronautical channel modeling," IEEE Transactions on Vehicular Technology, vol. 51, no. 2, pp. 254–264, 2002.
[45] R. Sun and D. W. Matolak, "Air –ground channel characterization for unmanned aircraft systems part ii: hilly and mountainous settings," IEEE Transactions on Vehicular Technology, vol. 66, no. 3, pp. 1913–1925, Mar. 2017.

This article has been accepted for publication in a future issue of this journal, but has not been fully edited. Content may change prior to final publication. Citation information: DOI 10.1109/ACCESS.2018.2791098, IEEE Access

DONATELLA DARSENA (M'06-SM'16) received the Dr. Eng. degree *summa cum laude* in telecommunications engineering in 2001, and the Ph.D. degree in electronic and telecommunications engineering in 2005, both from the University of Napoli Federico II, Italy.

From 2001 to 2002, she was an engineer in the Telecommunications, Peripherals and Automotive Group, STMicroelectronics, Milano, Italy. Since 2005, she has been an Assistant Professor with the Department of Engineering, University of Napoli Parthenope, Italy. Her research activities lie in the area of statistical signal processing, digital communications, and communication systems. In particular, her current interests are focused on equalization, channel identification, narrowband-interference suppression for multicarrier systems, space-time processing for cooperative communications systems and cognitive communications systems, and software-defined networks. Dr. Darsena has served as an Associate Editor for the IEEE COMMUNICATIONS LETTERS since December 2016.

GIACINTO GELLI was born in Napoli, Italy, on July 29, 1964. He received the Dr. Eng. degree *summa cum laude* in electronic engineering in 1990, and the Ph.D. degree in computer science and electronic engineering in 1994, both from the University of Napoli Federico II.

From 1994 to 1998, he was an Assistant Professor with the Department of Information Engineering, Second University of Napoli. Since 1998 he has been with the Department of Electrical Engineering and Information Technology, University of Napoli Federico II, first as an Associate Professor, and since November 2006 as a Full Professor of Telecommunications. He also held teaching positions at the University Parthenope of Napoli. His research interests are in the broad area of signal and array processing for communications, with current emphasis on multicarrier modulation systems and space-time techniques for cooperative and cognitive communications systems.

IVAN IUDICE was born in Livorno, Italy, on November 23, 1986. He received the B.S. and M.S. degrees in telecommunications engineering in 2008 and 2010, respectively, and the Ph.D. degree in information technology and electrical engineering in 2017, all from University of Napoli Federico II, Italy.

Since 2011, he has been part of the Electronics and Communications laboratory at Italian Aerospace Research Centre (CIRA), Capua, Italy. His research activities lie in the area of signal processing, array processing, digital communications and mobile communication systems. In particular, his current interests are focused on developing communication techniques optimized for aerospace environments.

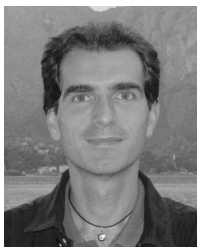

FRANCESCO VERDE (M'10-SM'14) was born in Santa Maria Capua Vetere, Italy, on June 12, 1974. He received the Dr. Eng. degree *summa cum laude* in electronic engineering from the Second University of Napoli, Italy, in 1998, and the Ph.D. degree in information engineering from the University of Napoli Federico II, in 2002. Since December 2002, he has been with the University of Napoli Federico II. He first served as an Assistant Professor of signal theory and mobile communications and, since December 2011, he has served as an Associate Professor of telecommunications with the Department of Electrical Engineering and Information Technology. His research activities include orthogonal/non-orthogonal multiple-access techniques, space-time processing for cooperative/cognitive communications, wireless systems optimization, and software-defined networks.

Prof. Verde has been involved in several technical program committees of major IEEE conferences in signal processing and wireless communications. He has served as an Associate Editor of the IEEE SIGNAL PROCESSING LETTERS since 2014 and IEEE TRANSACTIONS ON COMMUNICATIONS since 2017. He was an Associate Editor of the IEEE TRANSACTIONS ON SIGNAL PROCESSING from 2010 to 2014 and a Guest Editor of the EURASIP Journal on Advances in Signal Processing in 2010. He is an elected member of the IoT Special Internet Group (SIG) of the IEEE Signal Processing Society from 2018 to 2020.